

EXPERIMENTAL INVESTIGATION OF THE DYNAMIC STABILITY DERIVATIVES FOR A FIGHTER MODEL

M.R. Soltani*, Ali R. Davari**

*Associate Professor, **PhD. Student

Department of Aerospace Engineering, Sharif University of Technology
H. Ebnoddin, H., Head of Qhadr Aerodynamic Research Center
Tehran, I.R.Iran

Keywords: *Pitch Damping, Oscillation, Dynamic Stability*

Abstract

Extensive wind tunnel tests have been conducted to study the unsteady aerodynamic behavior of a standard dynamics model, SDM, oscillating in both pitch and plunge modes. Up to now, there is little or no result on the plunging behavior of an aircraft or missile as a whole and the present experiments can be considered as one of the first attempts to study the compressible flowfield over an aircraft undergoing both pitching and plunging motions. The experiments involved measuring the normal force and pitching moment of the model for the aforementioned motions at Mach numbers of 0.4, 0.6 and 1.5 and oscillation frequencies of 1.25, 2.77 and 6 Hz. The dynamic direct derivatives were then calculated from the measured data. The pitching results have been compared with the available data on the same model and good agreement has been achieved.

1 Introduction

The continuing demand for increased maneuverability of combat aircraft have brought dynamic stability problems to the forefront [1]. The unsteady flowfield on an aircraft in oscillatory motion is still characterized by unpredictable responses and as a result, there is considerable interest in dynamic direct and cross derivatives. Extensive wind tunnel tests have been conducted on different fighter configurations to study the unsteady aerodynamic derivatives [2]. Among these models, the Standard Dynamic Model (SDM)

was the one that has been tested in several research centers all over the world. Although numerous results on SDM have been published [3-5], there is still insufficient information about its stability derivatives especially in high subsonic and supersonic regimes at high frequencies. This paper addresses some of the most important aspects of dynamic stability of SDM oscillating in pitch and plunge in both subsonic and supersonic regimes. The experiments have been conducted at $M=0.4$, 0.6 and 1.5 and at the oscillation frequencies of 1.25, 2.77 and 6 Hz. This investigation involves the effects of Mach number and oscillation amplitude as well as oscillation frequency on the dynamic derivatives at low to moderate angle of attacks.

2 Model and Experimental Apparatus

The model considered in the present experiments was typical of a fighter aircraft called the standard dynamics model (SDM) and has been used in many research centers for flowfield study and verification of dynamic test rigs for several years [3-5]. It is a simplified model of the F-16 aircraft and is equipped with leading edge extensions (LEX), ventral fins and air inlet. It has 32 cm length, 10.34 cm semi span and is made of steel. Figure 1 shows this model. The experiments were conducted in the wind tunnel of Qhadr Research Center, Tehran. It is a continuous open circuit tunnel with test section dimensions of $60 \times 60 \times 120 \text{ cm}^3$. The test

section Mach numbers vary from 0.4 to 2.2 via the engine RPM and different nozzle settings.

Static, direct and cross coupling derivatives in pitch and plunge mode at various frequencies, Mach numbers and mean angles of attack were measured. Both static and oscillatory data were taken at Mach numbers of 0.4, 0.6 and 1.5, corresponding to the Reynolds numbers of 0.84, 1.26 and 3.15×10^7 per meter respectively. For pitching motion, the mean angle of attack ranged from 0 to 15 degrees. The oscillatory data were taken at oscillation amplitudes of ± 1 and ± 5 degrees and frequencies of 1.25, 2.77 and 6 Hz. For plunging motion, the static angles of attack were 0, 6 and 12 degrees and the plunging amplitudes were ± 1 , ± 3 and ± 5 cm with the same oscillation frequencies as those of the pitching motion, i.e. 1.25, 2.77 and 6 Hz. The oscillation system for the present experiments uses a crankshaft to convert the circular motion of the motor to reciprocal motion, which is transferred to the model by means of rods. This system can oscillate the model with frequencies ranging from 1 to 8 Hz.

Dynamic oscillatory data presented here are an average of several cycles at a sample rate based on the oscillation frequency. Various data acquisition rates were examined to find the best combination, which would provide as many cycles of quality data as possible. Raw data were then digitally filtered using a low-pass filtering routine. During the filtering process, cut off and transition frequencies were varied until the deviation between the original and the filtered data was a minimum. The dynamic derivatives for both pitching and plunging motions were then calculated at the specified mean angle of attack assuming that all the variations were linear about the mean angle of attack.

3 Results and Discussion

As mentioned before, the model was tested under both pitching and plunging motions. To author's knowledge no data is available in the literatures for plunging motion of the Standard Dynamics Model or another similar model. However some experimental results for this

model undergoing pitching motion are available, [3-5] and the present pitching results have been compared with them. Figures 2 and 3 show variations of the slope of the normal force coefficient ($C_{N\alpha}$) and pitch-damping derivative ($C_{m_{q+\dot{\alpha}}}$) with angle of attack. It should be noted that the present experimental setup is limited to moderate angle of attacks (15° at most). As is seen, good agreements are achieved verifying the accuracy of the measured parameters. This comparison also indicates that the experimental set up as well as data acquisition system and data corrections and reduction schemes are correct. From figure. 2 note that $C_{N\alpha}$ first reaches its maximum value at about 5 degrees angle of attack. Beyond this angle, it decreases drastically indicating flow separation over the wing surface. The normal force slope then continues to decrease until an angle of attack of about 10° . By further increasing the angle of attack, $C_{N\alpha}$ starts to increase again. The experimental data of ref. [6] indicate that for a delta wing with a leading edge sweep of about 70° the leading edge vortices start to form at an angle of attack of about 10° . These vortices create additional lift known as vortex lift. The strakes of the present model have a leading edge sweep of about 73° . Thus increase in $C_{N\alpha}$ beyond 10 degrees angle of attack shown in figure 2 is probably due to formation of the strake vortices. According to this figure, $C_{N\alpha}$ increases until an angle of attack of about 15° . This increase in $C_{N\alpha}$ is due to the strength of the strake vortices even though the flow over the main portion of the wing is probably separated. As mentioned before the present experimental setup for dynamic tests was limited to a mean angle of attack of about 14 deg. As seen from this figure, the variations of $C_{N\alpha}$ with α for the range of angles of attack tested compare well with those of ref. [3-5].

Figure 3 compares variations of the present pitch damping derivative result with other findings. Again within the ranges of α tested, the data compares well with those of ref. [3-5]. From this figure, it is seen that the pitch damping derivative continuously decreases as the angle of attack is increased, an indication of

a dynamically stable condition. Beyond an angle of attack of 15° the reduction in dynamic stability is probably caused by the strake vortices breakdown location, which has reached tail surfaces hence decreasing the stability level.

Figure 4 shows the effects of oscillation frequency on normal force coefficient for a sinusoidal motion of the present model with amplitude of 5° and at two different mean angles of attack; 0 and 14° , and a constant Mach number of 0.6 . The experimental data shown in this figure is for the oscillation frequencies of 1.25 , 2.77 and 6 Hz. For the two mean angles shown, as the oscillation frequency increases, both the slope and width of the hysteresis loop decrease. At $f=1.25$ Hz, the difference between the motion of the model and the flowfield around it at any instantaneous angle of attack creates the hysteresis loop in C_N . As the oscillation frequency increases, the phase difference between the motion and the corresponding flow around the model decreases. Thus the width and shape of the hysteresis loop differs from that of $f=1.25$ Hz case. At $f=6$ Hz, the flow no longer follows the motion. Consequently the upstroke and down stroke curves collapse on each other and C_N has a nearly constant value for the range of angle of attack tested. At higher mean angles of attack, formation of the vortices, their growth and probably breakdown have a strong effect on all aerodynamic coefficients. Comparing figures 4(a) with 4(b) it is clearly seen that the width and shape of the hysteresis loops vary with the mean angle of attack. The difference in hysteresis loop is probably caused by the formation of the strake vortices and their variation with angle of attack [7-9].

In addition to pitching tests as mentioned above, the experiments have been conducted for plunging motions with the same Mach numbers and oscillation frequencies as those of the pitching maneuvers. Figure 5 shows effects of the plunging frequency on variations of the normal force coefficient with vertical displacement of the model at two mean angles of attack of 0 and 12 degrees. As can be seen, at zero mean angles of attack, figure 5(a), the hysteresis loops of C_N are nearly identical for

both frequencies of 1.25 and 2.77 Hz. Note that the vertical velocity of the model is very small compared to the free stream Mach number. Hence the induced angle of attack due to this vertical displacement is too small consequently the value of C_N is negligible for the three frequencies examined here. At 12 degrees angle of attack the value of C_N decreases with increasing the frequency from 1.25 to 2.77 Hz as shown in figure 5(b). From this figure it is seen that for both cases shown here, $\alpha_{\text{mean}}=0$ and 12 degrees, the hysteresis in C_N disappears for the highest frequency, $f=6$ Hz. Further note that for all frequencies examined here C_N has higher values when plunged about the mean angle of 14 degrees but the width of the loops are almost the same for both mean angles of attack.

Figure 6 shows variations of the dynamic normal force slope, $C_{N\alpha}$, with mean angle of attack for pitching motion with oscillation frequencies of 1.25 and 2.77 Hz, Mach numbers of 0.4 and 0.6 and two different oscillation amplitudes of 1 and 5 degrees. Static values for both cases are also shown for comparison. According to figure 6(a), $C_{N\alpha}$ increases as the Mach number increases from 0.4 to 0.6 . The jump from $M=0.4$ to $M=0.6$ is probably due to the compressibility effects. Note that at $M=0.6$, some transonic regions may exist on the body, wing surfaces, etc. Further from this figure it can be seen that the effect of oscillation amplitude at $M=0.4$ is not significant.

At $M=0.6$ and amplitude of 5 degrees, the reduction in $C_{N\alpha}$ for all mean angles of attack is probably caused by the transonic region and occurrence of shock wave on the model. It seems that the shock strength increases at higher angles of attack, causing further reduction in $C_{N\alpha}$. Hence at $M=0.6$, the difference between amplitudes of 1 and 5 degrees, increases as the angle of attack is increased. Further, note that the values of dynamic normal force slope, $C_{N\alpha}$, at Mach number of 0.4 for both amplitudes 1 and 5 degrees agree well with the corresponding static values at the same Mach number up to the angle of attack of about 8 degrees beyond which, the static value of $C_{N\alpha}$ continues to decrease but it's dynamic value for both amplitudes increases slightly. This is probably

due to the separation point on the wing surface that has been delayed by the dynamic motion of the model. For Mach number of 0.6, the difference between static and dynamic $C_{N\alpha}$ is considerable, which is probably due to the impact of unsteady motion on the effects of compressibility at this Mach number.

Effects of Mach number and oscillation amplitude for oscillation frequency of 2.77 Hz are shown in figure 6(b). Here the trend is similar to that of figure 6(a). Again for all Mach numbers and angles of attack shown here, as the Mach number increases, $C_{N\alpha}$ increases too. Also for the oscillation frequency of 2.77 Hz, the magnitude of $C_{N\alpha}$ for both Mach numbers of 0.4 and 0.6 is slightly lower than those in figure 6(a). As mentioned before, at high oscillation frequencies, the phase difference between the motion and the corresponding flow around the model decreases and consequently the width and slope of the hysteresis loop is decreased. [8,9]. This phenomenon can be seen by inspecting the pitching C_N data shown in figure 4.

At Mach number of 0.6 and frequency of 2.77 Hz for all angles of attack, $C_{N\alpha}$ increases as the oscillation amplitude increases. This is opposed to that of the frequency of 1.25 Hz shown in figure 6(a). This phenomenon is probably caused by the effect of oscillation on the formation of the unsteady shock systems established on the model in the transonic regime. In this regime the shock waves are not in a fixed position on the body and move back and forth with time. At supersonic Mach numbers, the shock system is nearly attached to the body and does not change its position continuously. For the present model, SDM, when the unsteady pitching motion is imposed to the flow with Mach numbers between 0.6 and 1.2, the motion of the shock system on the model increases. This may push the unsteady shocks to the downstream of the model and vary its position on the body with angle of attack. For Mach number of 1.5 and amplitude of 1 degree, $C_{N\alpha}$ is nearly constant up to the angle of attack of about 6 degrees. It starts to decrease at higher angles of attack while for the oscillation amplitude of 5 degrees, $C_{N\alpha}$ is nearly constant

up to 4 degrees angle of attack and reduces sharply at higher angles of attack. This is due to the different shock structure forming over and below the model and its variations with the angle of attack. As figure 6(b) shows, for the frequency of 2.77 Hz in contrast with the case of $f=1.25$ Hz, for $M=0.4$, the dynamic $C_{N\alpha}$ is obviously less than the static one and for $M=1.5$, the dynamic $C_{N\alpha}$ is more than its corresponding static value. At $M=0.6$, the values of static $C_{N\alpha}$ lies between the dynamic values for 1 and 5 degrees oscillation amplitude.

In figure 7 effects of the amplitude and frequency on $C_{N\alpha}$ at Mach number of 0.4 is shown. As stated before, at Mach number of 0.4, oscillation amplitude does not have significant effect on $C_{N\alpha}$. Again as the oscillation frequency increases, $C_{N\alpha}$ decreases. Also as was discussed earlier, the values of $C_{N\alpha}$ at oscillation frequency of 1.25 Hz are much closer to those of the static one, while there is a considerable difference between the dynamic $C_{N\alpha}$ at the oscillation frequency of $f=2.77$ Hz and the corresponding static values. At moderate to high angles of attack, where the flow separates over the wing surface, it seems that the dynamic and static values of $C_{N\alpha}$ collapse on each other. However as mentioned before, the present experiments were restricted to the mean angles of attack up to 14 degrees.

Figure 8 shows effects of oscillation amplitude and frequency on the static stability behavior of the model for Mach number of 0.4. The static data are also shown for comparison. According to this figure for both frequencies, the static stability decreases as the oscillation amplitude increases. Also dynamic $C_{m\alpha}$ for the frequency of 1.25 Hz shows a more stable attitude than the static case. However due to the aforementioned phenomena, static stability level decreases considerably as the oscillation frequency increases.

Figure 9 shows variations of the dynamic pitching moment slope, $C_{m\alpha}$, with mean angle of attack for oscillation frequencies of 1.25 and 2.77 Hz, the Mach numbers of 0.4 and 0.6 and two different oscillation amplitudes of 1 and 5 degrees. The trend is similar to that of $C_{N\alpha}$ in figure 6. At Mach number of 0.4 the dynamic

values of $C_{m\alpha}$ are closed to the static ones up to the angle of attack of about 8 degrees, figure 9(a), while at Mach number of 0.6 the absolute value of dynamic $C_{m\alpha}$ increases considerably comparing to its corresponding static values. The static stability of the model at Mach number of 0.6 is better than that of $M=0.4$ due to the compressibility effects. Further, the effect of oscillation amplitude at Mach number of 0.4 is less than that at Mach number of 0.6, indicating the effects of transonic flow at this Mach number on the static stability.

In figure 9(b) for the oscillation frequency of 2.77 Hz the effects of Mach number and oscillation amplitude are more pronounced than those for the frequency of 1.25 Hz. Similar to the case of $C_{N\alpha}$, the absolute values of dynamic $C_{m\alpha}$ at $M=0.4$ are lower and at $M=1.5$ are higher than their static counterparts. This implies that the static stability of the model increases as the Mach number increases. However at supersonic conditions, $M=1.5$, for both oscillation amplitudes, the static stability linearly decreases for angles of attack greater than 4 degrees.

Variations of the Normal force damping coefficient, $C_{N_{q+\dot{\alpha}}}$, with mean angle of attack for three Mach numbers of 0.4, 0.6 and 1.5, two oscillation frequencies of 1.25 and 2.77 and two oscillation amplitudes of 1 and 5 degrees are shown in figure 10. For the frequency of 1.25 Hz, figure 10(a) shows that as the mean angle of attack increases, the value of $C_{N_{q+\dot{\alpha}}}$ increases too, except for a region between the angle of attack of 4 and 8 degrees for $M=0.4$. Also the dynamic normal force damping coefficient, $C_{N_{q+\dot{\alpha}}}$, decreases with increasing the oscillation amplitude. This figure also shows that the rate of increase of $C_{N_{q+\dot{\alpha}}}$ for $M=0.6$ is much more than that of $M=0.4$ which has a nearly constant value, indicating a desirable behavior for normal force damping of the model in transonic flow regime. Further for both Mach numbers, $M=0.4$ and 0.6, figure 10(a) shows that beyond 12 degrees angles of attack, the difference between $C_{N_{q+\dot{\alpha}}}$ for both cases $\alpha_A = 1$ and 5 degrees, seems to diminish. In figure 10(b), variations of the Normal force damping

coefficient, $C_{N_{q+\dot{\alpha}}}$, with mean angle of attack for the oscillation frequency of 2.77 Hz is shown. At this frequency, the values of $C_{N_{q+\dot{\alpha}}}$ are less than those for the frequency of 1.25 Hz shown in figure 10(a). As discussed before, this is due to the decrease in phase difference between the model motion and the instantaneous flow field around it. Further by inspecting this figure, a dramatic linear increase in $C_{N_{q+\dot{\alpha}}}$ at Mach number of 1.5 is observed while for the two subsonic Mach numbers, this derivative reaches to a steady state value at moderate to high angles of attack.

Figure 11 shows variations of damping in pitch derivative, $C_{m_{q+\dot{\alpha}}}$, with angle of attack for three Mach numbers of 0.4, 0.6 and 1.5, two oscillation frequencies of 1.25 and 2.77 and two oscillation amplitudes of 1 and 5 degrees. Note that the dynamic stability increases as the oscillation amplitude increases, which is in contrast with the results for $C_{m\alpha}$ case shown in figure 9 where the static stability has been shown to decrease with increasing the oscillation amplitude. This is due to the strong effect of oscillation amplitude on oscillation time history and hence on $\dot{\alpha}$ and q . According to figure 11(a), effects of oscillation amplitude is more pronounced at $M=0.6$ than $M=0.4$, which is due to the transonic regions on the body at $M=0.6$. Also the dynamic stability at $M=0.4$ has a gentle increasing rate with increasing mean angle of attack while for $M=0.6$, this rate is more pronounced. This is probably due to shock effects, which may be diminished on the body as the mean angle of attack increases. Figure 11(b) shows similar trends for the oscillation frequency of 2.77 Hz. Here the rate of increase of the dynamic stability at the supersonic speed, $M=1.5$, is much more than the other two Mach numbers. For the Mach number of 0.4, the dynamic stability is nearly constant throughout the mean angles of attack tested. At $M=0.6$, the dynamic stability is nearly constant up to the angle of attack of about 6 degrees beyond which it increases linearly with increasing angle of attack, which is the onset of transonic flow regions on the body. At $M=1.5$, for 1 degree

amplitude, the pitch damping increases linearly with mean angle of attack. As stated before, along with the pitching data presented here, experiments were conducted on plunging motion of the standard Dynamics Model, SDM, at the same Mach numbers and oscillation frequencies as those for the pitching motion. The plunging experiments have been carried out for three static angles of attack of 0, 6 and 12 degrees. The dynamic derivatives responsible for plunging motions are $C_{N\alpha}$, $C_{N\dot{\alpha}}$, $C_{m\alpha}$ and $C_{m\dot{\alpha}}$. However due to page limitation only the derivative $C_{N\dot{\alpha}}$ will be presented here as the plunging results.

Figure 12 compares the normal force damping derivatives in pitching and plunging motions for $M=0.4$, two oscillation frequencies of 1.25 and 2.77 Hz, two pitching amplitudes of 1 and 5 degrees and three plunging amplitudes of 1, 3 and 5 cm. Variations of $C_{N_{q+\dot{\alpha}}}$ has been explained before. From figure 12(a) it is evident that for the frequency of 1.25 Hz and Mach number of 0.4, almost half of the normal force damping is due to $\dot{\alpha}$ i.e. $C_{N\dot{\alpha}}$ is about half of the $C_{N_{q+\dot{\alpha}}}$ hence the remainder will be the contribution of pure C_{Nq} . In plunging motion, as the static angle of attack increases, $C_{N\dot{\alpha}}$ increases up to an angle of attack of 6 degrees. It should be noted that the maximum value of $C_{N\dot{\alpha}}$ may not necessarily occur at this angle. However the plunging experiments have been conducted for the three mean angles of 0, 6 and 12 degrees only. At angle of attack of 12 degrees $C_{N\dot{\alpha}}$ decreases due to the flow separation over the model. Figure 12(b) shows variation of $C_{N\dot{\alpha}}$ from the plunging and $C_{N_{q+\dot{\alpha}}}$ from the pitching motions for the oscillation frequency of 2.77 Hz. Contrary to the case of $f=1.25$ Hz in Figure 12(a), it is evident that for the frequency of 2.77 Hz, the values of $C_{N\dot{\alpha}}$ are of the same order of magnitude as $C_{N_{q+\dot{\alpha}}}$, hence C_{Nq} has a very small contribution to the normal force damping derivative, $C_{N_{q+\dot{\alpha}}}$ for this frequency. Note that C_{Nq} is mainly

due to the flow upwash and downwash effects while $C_{N\dot{\alpha}}$ is due to variations of the effective angle of attack. It can be seen by inspection that at higher oscillation frequencies the upwash and downwash effects almost diminish, which means that the flow cannot follow the motion as it did at lower frequencies. This phenomenon is probably the main reason for reducing the dynamic $C_{N\alpha}$ as explained in references 8 and 9.

4 Conclusion

Extensive wind tunnel tests have been conducted to study the unsteady aerodynamic behavior of a standard dynamics model oscillating in pitch and plunge. The experiments involved measuring the normal force and pitching moments of the model in both pitching and plunging motions. The dynamic derivatives for both motions were calculated using the acquired data. The results show that in a pitching motion, the width of the loop and slope of the normal force and pitching moment decreases as the frequency increases. Also for the cases examined here, both the static and dynamic stability of the model during pitching motion increase as the Mach number increases from 0.4 to 1.5 but the rate of increase at $M=1.5$ is much higher than the two other cases. The results for plunging motion show that since the vertical velocity during oscillation is negligible comparing to the free stream velocity, the induced angle of attack and hence the normal force due to the plunging is too small. Also the normal force damping coefficients have shown that for $f=1.25$ Hz the damping in plunge is of the same order as damping in pitch but for higher frequency i.e. $f=2.77$ Hz, $C_{N\dot{\alpha}}$ is smaller than $C_{N_{q+\dot{\alpha}}}$, which the difference between them can be considered as the pure pitching C_{mq} contribution.

5 Acknowledgement

The authors would like to express their sincere thanks to the Iranian AIO especially the vice chairman of the education and research department for financial support of this project.

EXPERIMENTAL INVESTIGATION OF THE DYNAMIC STABILITY DERIVATIVES FOR A FIGHTER MODEL



Figure 1- The Standard Dynamic Model (SDM)

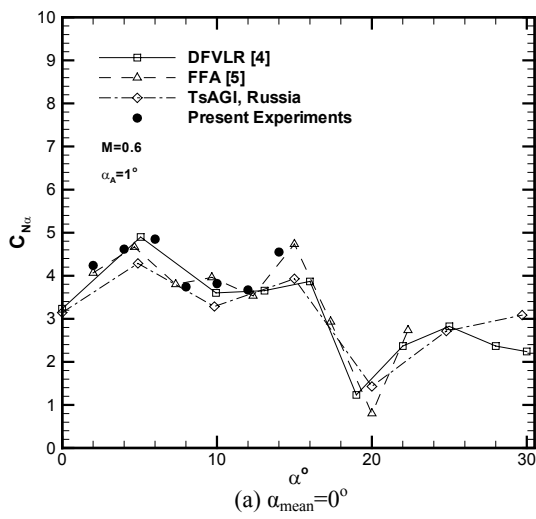


Figure 2- variations of dynamic normal force

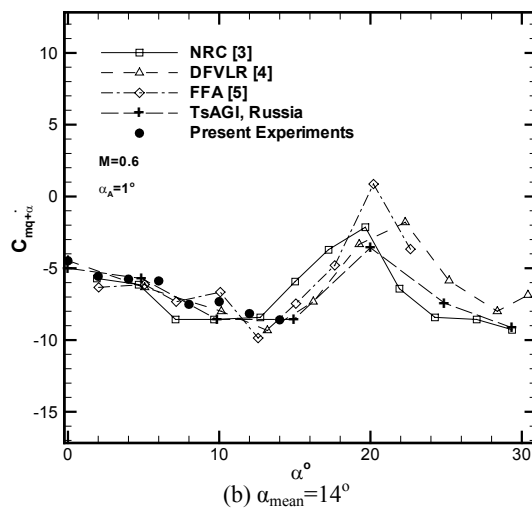


Figure 3- variations of the pitch damping derivative

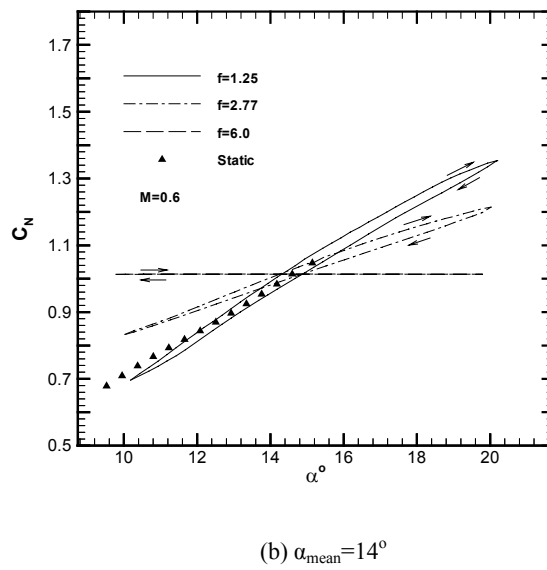
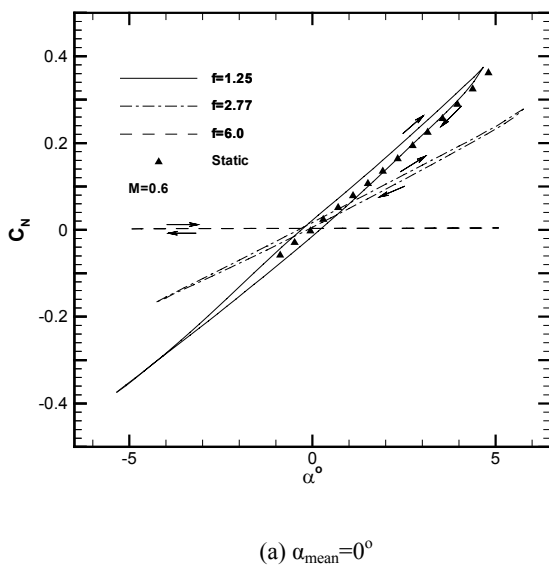


Figure 4- Effects of oscillation frequency on variations of normal force with angle of attack in pitching motion

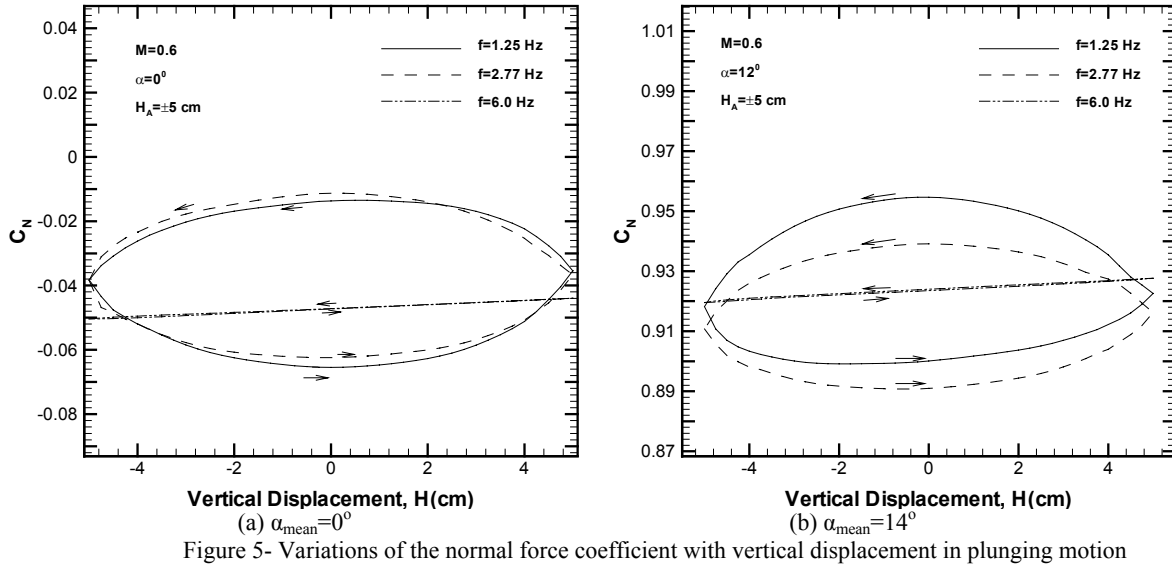


Figure 5- Variations of the normal force coefficient with vertical displacement in plunging motion

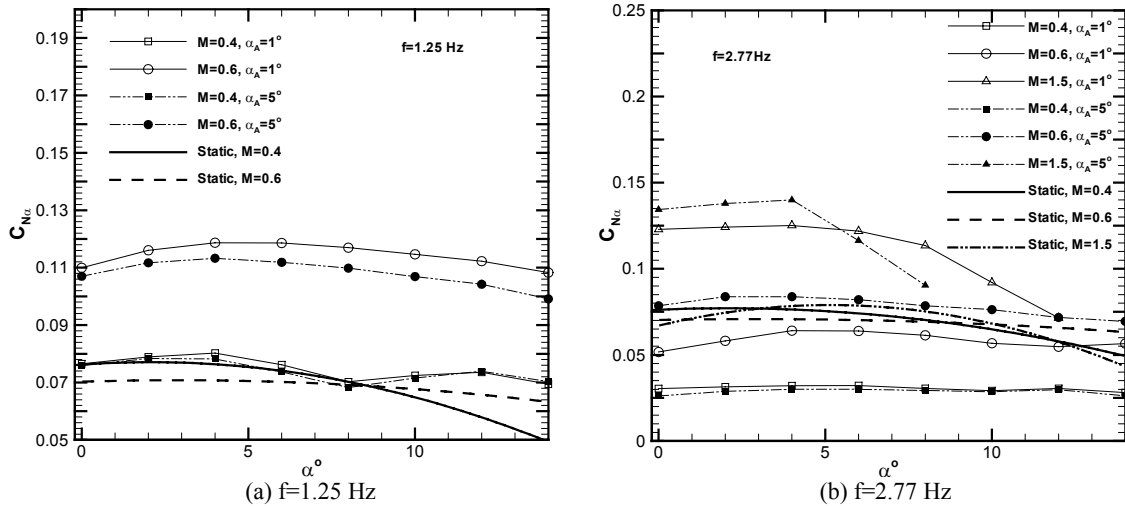


Figure 6- Variations of the normal force slope with mean angle of attack

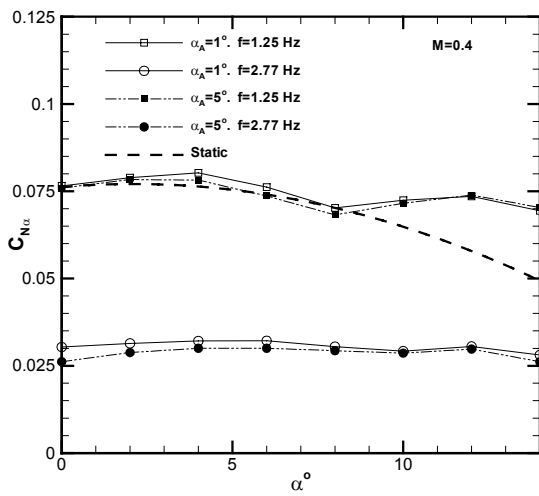


Figure 7- Effects of oscillation frequency and Mach number on variations of dynamic normal force slope with mean angle of attack

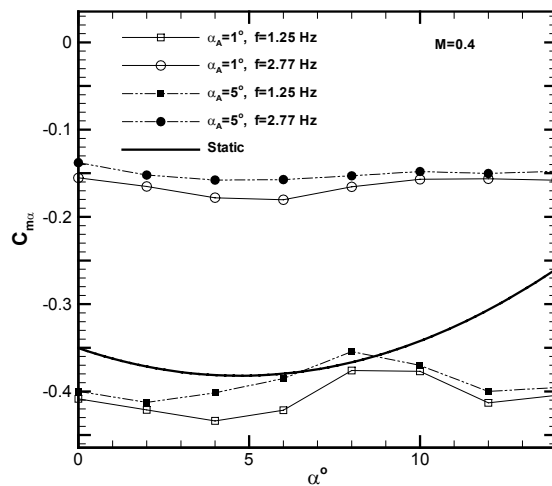
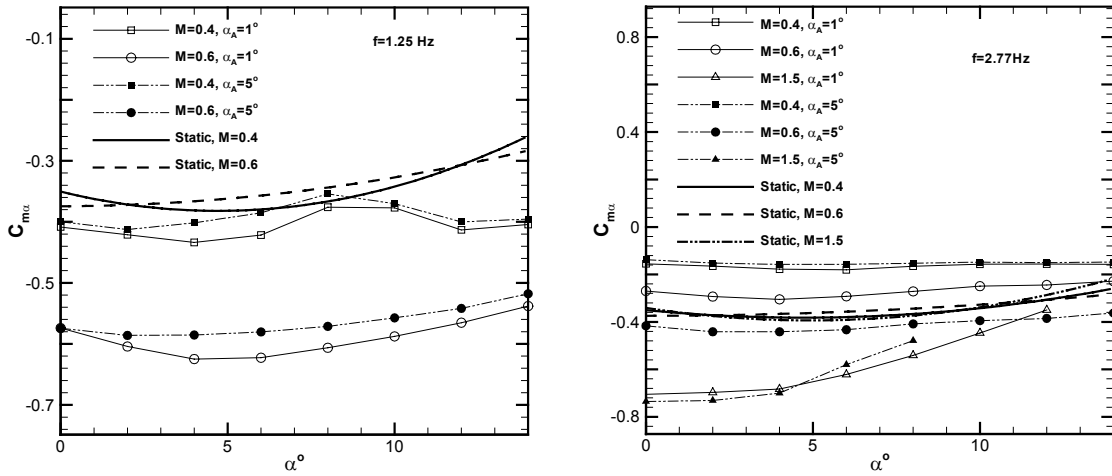
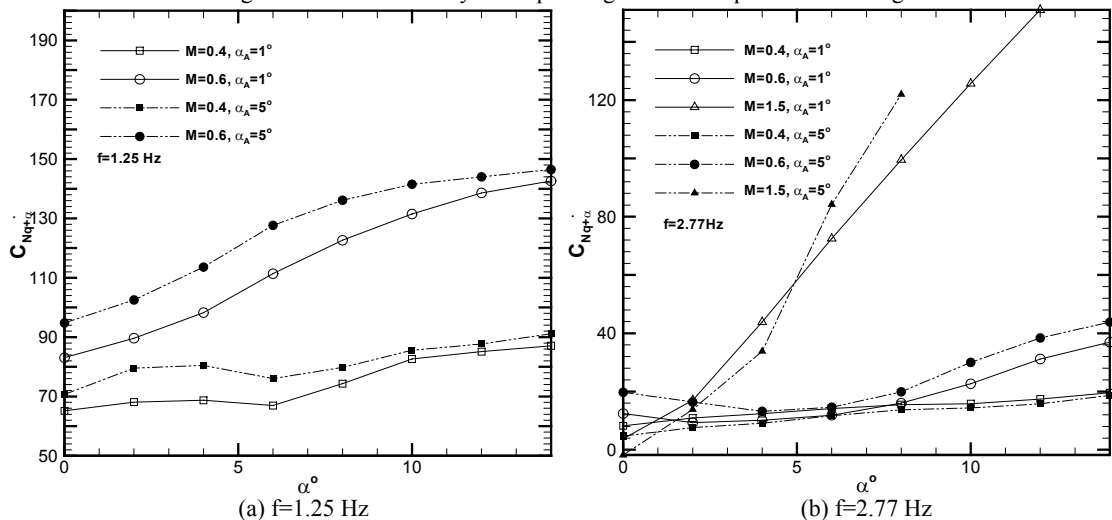


Figure 8- Effects of oscillation frequency and Mach number on variations of dynamic pitching moment slope with mean angle of attack

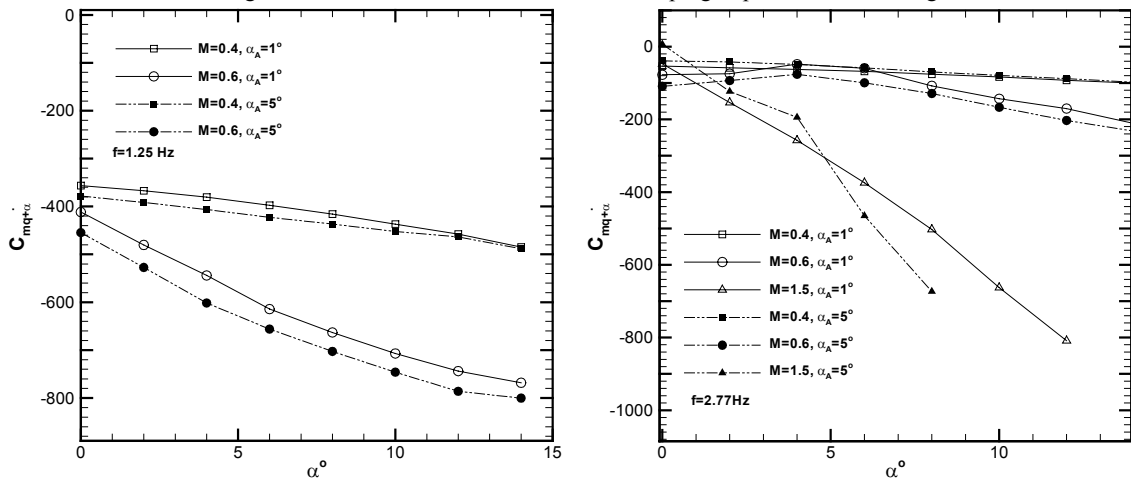
EXPERIMENTAL INVESTIGATION OF THE DYNAMIC STABILITY DERIVATIVES FOR A FIGHTER MODEL



(a) $f=1.25$ Hz (b) $f=2.77$ Hz
Figure 9- Variations of dynamic pitching moment slope with mean angle of attack



(a) $f=1.25$ Hz (b) $f=2.77$ Hz
Figure 10- Variations of the normal force damping in pitch with mean angle of attack



(a) $f=1.25$ Hz (b) $f=2.77$ Hz
Figure 11- Variations of pitch damping derivative with mean angle of attack

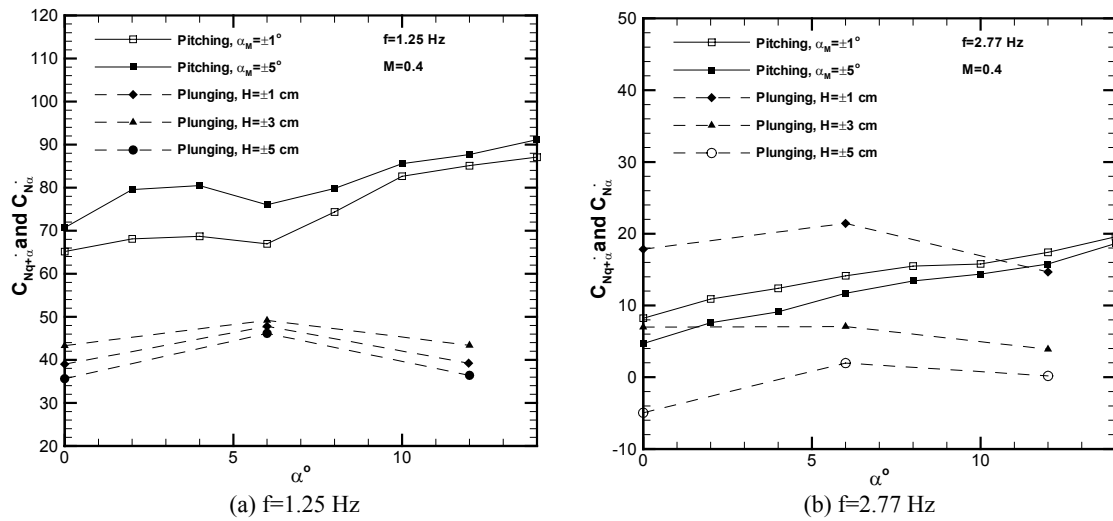


Figure 12- Comparison of the normal force damping in pitch and plunge

REFERENCES

- [1] Beyers, M.E., "Free Flight Investigation of High-Maneuverability Missile Dynamic," *Journal of Spacecraft and Rockets*, Vol. 14, No. 4, April 1975, pp. 224-230
- [2] Orlik-Rückeman, K.J., "Aerodynamic Aspects of Aircraft Dynamics at High Angles of Attack," *Journal of Aircraft*, Vol. 20, No. 9, Sept. 1983, pp.737-751
- [3] Beyers, M.E., "SDM Pitch and Yaw Axis Stability Derivatives," AIAA Paper 85-1827, 1985.
- [4] Schmidt, E., "Standard Dynamics Model Experiments With the DFVLR/AVA Transonic Derivative Balance," AGARD CP-386, May 1985.
- [5] Jansson, T. and Torngren, L., "New Dynamic Testing Techniques and Related Results at FFA," AGARD CP-386, May 1985.
- [6] Wentz, W.H., Wind Tunnel Investigations of Vortex Break Downs, Ph.D. Dissertation, University of Kansas, Lawrence, KS, 1968.
- [7] Soltani, M.R., Ebrahimi, S.A., Davari, A.R., "A simple analytical method for predicting the amplitude and frequency of a delta wing model undergoing rocking motion," AIAA Paper 2002-0710, March 2002.
- [8] Soltani, M.R, Davari, A.R., "A New Method Based on Neural Network To Predict the Unsteady Aerodynamic Behavior of Two Different Models Undergoing Pitching Motion," *submitted to the Journal of Aircraft*, Sep. 2003
- [9] Soltani, M.R, Davari, A.R., "Identification of a New Similarity Parameter to Investigate the Unsteady Aerodynamic Behavior of an Aircraft in Pitching Motion," *submitted to The Royal Aeronautical Journal*, Nov. 2003.